

Sol-gel Combustion Synthesis, Structural and Optical Band Gap Energy Study of $Zn_{0.85}Ni_{0.1}Mg_{0.05}Fe_2O_4$ Nanoparticles

Shimelis Adem Abegaz

Department of Physics, College of Natural Sciences, Arba Minch University, Arba Minch, Ethiopia

Abstract- This study reports the synthesis of $Zn_{0.85}Ni_{0.1}Mg_{0.05}Fe_2O_4$ nanoparticles by using a sol-gel combustion method using the raw materials $Zn(NO_3)_2 \cdot 6H_2O$, $Ni(NO_3)_2 \cdot 6H_2O$, $Mg(NO_3)_2 \cdot 6H_2O$, $Fe(NO_3)_3 \cdot 9H_2O$ and $C_6H_8O_7 \cdot H_2O$. The synthesized $Zn_{0.85}Ni_{0.1}Mg_{0.05}Fe_2O_4$ sample was characterized by X-ray powder diffraction (XRD), Fourier transform infrared (FTIR) spectroscopy and ultraviolet-visible (UV-vis) spectroscopy. Using these techniques, the structure as well as the optical property of the synthesized sample were investigated. The lattice parameter, unit cell volume and band gap of $Zn_{0.85}Ni_{0.1}Mg_{0.05}Fe_2O_4$ sample were also estimated. The XRD analysis confirmed that the synthesized $Zn_{0.85}Ni_{0.1}Mg_{0.05}Fe_2O_4$ sample possessed a single-phase cubic spinel structure with Fd-3m space group. The lattice parameter, the unit cell volume and the average crystal size of $Zn_{0.85}Ni_{0.1}Mg_{0.05}Fe_2O_4$ sample were found to be 0.8342 nm, 580.5 (\AA)³ and 51 nm, respectively. The FT-IR analysis of $Zn_{0.85}Ni_{0.1}Mg_{0.05}Fe_2O_4$ sample confirms the presence of two strong absorption bands ν_1 and ν_2 which lie in the expected range of cubic spinel-type ferrite material. It also revealed the presence of the tetrahedral and octahedral sites in $Zn_{0.85}Ni_{0.1}Mg_{0.05}Fe_2O_4$ sample. The optical band gap of the sample was found to be 2.4 eV, indicating the semiconductor behavior of $Zn_{0.85}Ni_{0.1}Mg_{0.05}Fe_2O_4$ sample.

Keywords: Characterization, Sol-gel combustion, Structure Nanoparticle, Optical property.

1. INTRODUCTION

Iron based spinel ferrites belong to a special class of magnetic material consisting of metal oxide and ferric oxide as their main compositions. Spinel ferrites have some distinct magnetic, electric and dielectric properties, which made them more attractive to the current field of science and technology. These important properties of spinel ferrites find application in transformer core, sensors, magnetic switches, microwave devices, electromagnetic circuits, antenna rods and in the field of medicines [1-2]. Different researchers have reported that the structure, electrical, dielectric as well as dielectric properties of spinel ferrites largely dependent on the preparation method, chemical composition, the calcination as well as sintering temperature, grain size and surface morphology [3-7].

Spinel ferrites are represented by the formula MFe_2O_4 where "M" stands for divalent cations like Mg, Zn, Cu, Ni,

Mn, Cd etc. The divalent cation "M" can be replaced by other divalent metal ions and Fe^{3+} can also be replaced by other trivalent cations like In, Al, Cr, Ga etc. Spinel ferrites have cubic spinel structure with Fd3m space group [8]. The crystal structure possesses two interstitial sites namely tetrahedral (A) site and octahedral [B] site. They are also classified into the following three types on the basis of the distribution of cations in the tetrahedral site and octahedral site [B]: normal, inverse and random spinel ferrites [9]. A ferrite is called normal spinel when the divalent cations occupy the tetrahedral (A) sites while $2Fe^{3+}$ ions are at octahedral [B] site. $ZnFe_2O_4$ and $CdFe_2O_4$ belong to normal spinel in which the divalent cations Zn^{2+} or Cd^{2+} are located at the tetrahedral site, while Fe^{3+} ions are at the octahedral site. In the inverse spinel ferrites, half of the ferric ion Fe^{3+} in MFe_2O_4 is located at the tetrahedral site while the remaining Fe^{3+} and the divalent M^{2+} cation is located at the octahedral site. $NiFe_2O_4$ and $CoFe_2O_4$ belong to the normal spinel in which the divalent cations Ni^{2+} or Co^{2+} and half of Fe^{3+} cations are located at the octahedral site, while the remaining Fe^{3+} ions are at the tetrahedral site [10]. On the other hand, the divalent metal ions M^{2+} and trivalent Fe^{3+} ions are distributed at both tetrahedral and octahedral sites in random spinel ferrites ($MnFe_2O_4$).

In recent years, study of transition metal oxides based ferrites (MFe_2O_4) (M=Cu, Co, Ni and Zn) has gained substantial interest. Among them, $ZnFe_2O_4$ is the most extensive semiconductor magnetic material, where Zn^{2+} cations occupy tetrahedral sites and Fe^{3+} ions in the octahedral sites. This arrangement of cations can be represented using the relation $(Zn^{2+})[Fe_2^{3+}]O_4$. This ferrite material possesses a direct bulk band gap of 1.9 eV [11]. $ZnFe_2O_4$ ferrite is also chemically and thermally stable material suitable for a wide variety of applications including catalysts, photocatalysts, magnetic resonance imaging, magnetic material and drug delivery [12-17]. Recently, the nanoscale $ZnFe_2O_4$ based ferrite materials has been extensively studied by worldwide researchers, because of their unique size dependent physical and chemical properties as compared to the bulk sized materials.

Spinel ferrite materials in nano-size can be synthesized by using different synthesis methods. The structure and properties of spinel ferrites in bulk and nano-size form are different from each other due to size effect. Currently, the following wet chemical synthesis methods such as sol-gel, hydrothermal, co-precipitation method, sol-gel method and combustion are utilized to

synthesize spinel ferrites [18-23]. All these synthesis methods effectively affect the physical properties like structural, optical, electrical, dielectric, magnetic properties of spinel ferrites. In this study, $Zn_{0.85}Ni_{0.1}Mg_{0.05}Fe_2O_4$ sample was prepared by using sol-gel combustion method and its structure and optical band gap energy were investigated using X-ray powder diffraction, Fourier transform infrared spectroscopy and ultraviolet visible spectroscopy.

2. MATERIALS AND METHODS

2.1. Synthesis Procedures

All chemicals were of analytical grade and were used without further purification. $Zn_{0.85}Ni_{0.1}Mg_{0.05}Fe_2O_4$ sample in the form powder was synthesized by sol-gel combustion method using the raw materials Zinc nitrate hexahydrate ($Zn(NO_3)_2 \cdot 6H_2O$), Nickel nitrate hexahydrate ($Ni(NO_3)_2 \cdot 6H_2O$), Magnesium nitrate hexahydrate ($Mg(NO_3)_2 \cdot 6H_2O$) and Ferric nitrate nonahydrate ($Fe(NO_3)_3 \cdot 9H_2O$). Citric acid monohydrate ($C_6H_8O_7 \cdot H_2O$) was also used as a fuel and chelating agent. A stoichiometric amounts of raw materials $Zn(NO_3)_2 \cdot 6H_2O$, $Ni(NO_3)_2 \cdot 6H_2O$, $Mg(NO_3)_2 \cdot 6H_2O$ and $Fe(NO_3)_3 \cdot 9H_2O$ was dissolved in 40 ml double distilled water and stirred for about 10 minutes. A stoichiometric amount of citric acid was also dissolved in 30 ml distilled water in separate beaker and stirred for about 10 minutes. Further, the citric acid solution was then added in to the solution of nitrates, and the molar ratio of citric acid to total metal ions was 1:1. The resulting solution was mixed with a magnetic stirrer at $50^\circ C$ until a clear viscous gel occurs. Further, Ammonium solution was added slowly to this solution with constant stirring until pH 6 was achieved. To remove water, the sol was heated at $90^\circ C$ for about 3 hours. As the evaporation of water proceeded, the sol turned into a viscous gel. When the obtained gel was further heated at $90^\circ C$, combustion process was conducted in the hottest zones of the beaker and propagated to self-ignition from the bottom to the top like the eruption of a volcano, and he obtained black powder was ground in an agate mortar for about 2 hours. The resulting powder was calcined at $950^\circ C$ for 12 hours to obtain the spinel phase $Zn_{0.85}Ni_{0.1}Mg_{0.05}Fe_2O_4$ sample, and the sample was ground for an hour using an agate mortar and pestle. The detail of the synthesis procedure is shown in Fig. 1.

2.2. Material Characterizations

The structure as well as the phase formation of the synthesized sample were identified by an X-ray diffractometer (XRD-7000S diffractometer) with a $Cu K\alpha$ radiation of wavelength $\lambda = 1.5406 \text{ \AA}$ source. The measurement was conducted between a diffraction angle of $2\theta = 10^\circ$ and 80° . FT-IR spectroscopy measurement was

also conducted by IR AFFINITY-1S shimadzu instrument in transmittance method with potassium Bromide (KBr) as IR window in the wavenumber region of 400 to 4000 cm^{-1} . The optical band gap energy of the sample was also measure by using Uv-vis spectroscopy (Specord 50 plus instrument) in the wavelength range from 200 to 800 nm .

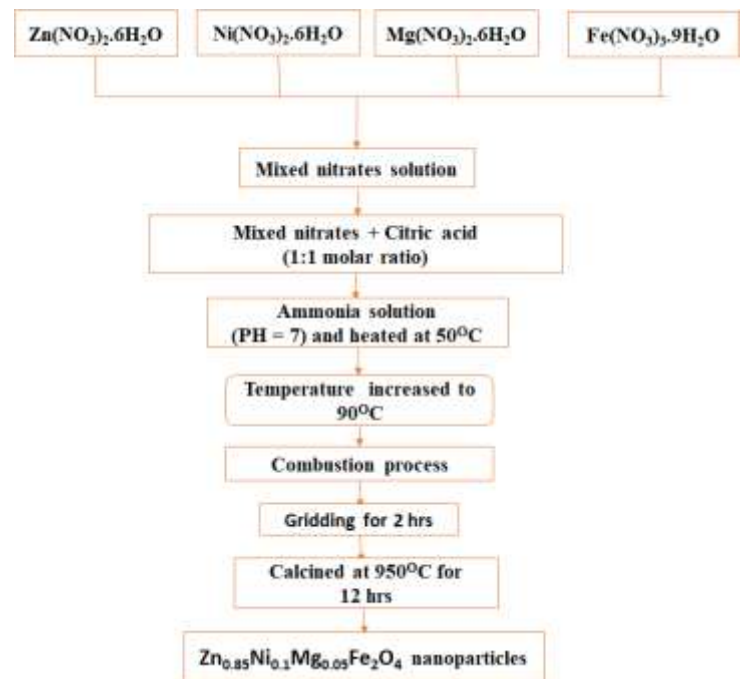


Figure-1: Flow chart of the sol-gel combustion synthesis procedure.

3. RESULTS AND DISCUSSION

3.1. XRD analysis

X-ray powder diffraction is a technique which is helpful for analyzing the phase formation and the structure of compounds. It is also important to estimate the crystalline size, lattice parameter and unit cell volume of compounds. The XRD pattern of $Zn_{0.85}Ni_{0.1}Mg_{0.05}Fe_2O_4$ sample which was prepared by using sol-gel combustion method and calcined at a temperature of $950^\circ C$ for 12 hours is shown in Fig. 2. As it is observed from the figure, broadened, sharp and well defined XRD peaks are observed in the synthesized samples, indicated that $Zn_{0.85}Ni_{0.1}Mg_{0.05}Fe_2O_4$ sample possesses good crystalline structure. The broadened peaks observed in the XRD analysis confirms the formation of monocrystalline $Zn_{0.85}Ni_{0.1}Mg_{0.05}Fe_2O_4$ sample. This is due to the fact that in nano sized particles there are insufficient diffraction centers, which causes the diffraction lines brooding.

As shown in the Fig.2, the indexed peaks (220), (311), (222), (400), (422), (511), (440), and (533) for synthesized sample confirm the formation of a single phase spinel cubic structured $Zn_{0.85}Ni_{0.1}Mg_{0.05}Fe_2O_4$ sample synthesized by combustion method using the raw materials $Zn(NO_3)_2 \cdot 6H_2O$, $Ni(NO_3)_2 \cdot 6H_2O$, $Mg(NO_3)_2 \cdot 6H_2O$ and $Fe(NO_3)_3 \cdot 9H_2O$. No additional phase formation is observed. The XRD peaks are also indexed using the Joint Committee on Powder Diffraction Standards (JCPDS) card with good agreement for $ZnFe_2O_4$ (card no. 89-4926). The obtained peaks from $Zn_{0.85}Ni_{0.1}Mg_{0.05}Fe_2O_4$ sample have a very good agreement with the reported results [6,13,24]. It is also reported that the Bragg planes of (422) and (440) correspond to tetrahedral and octahedral sites, respectively. In the XRD patterns, peaks of the plane of (422) and (440) are also identified, indicating the presence of the tetrahedral and octahedral sites in the $Zn_{0.85}Ni_{0.1}Mg_{0.05}Fe_2O_4$ sample.

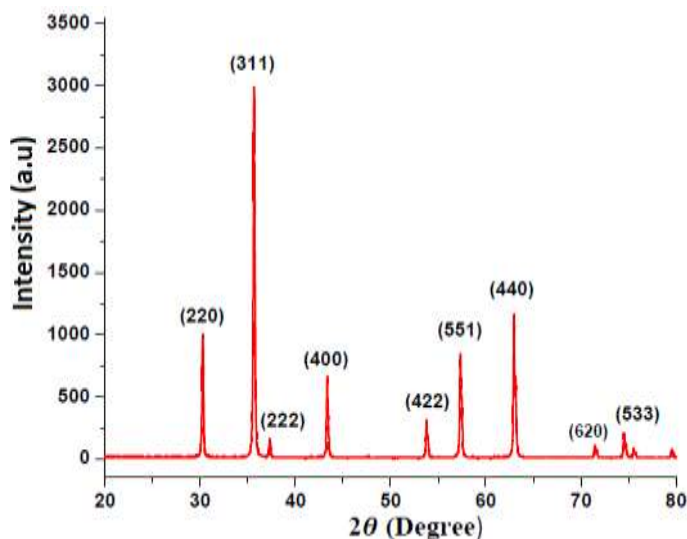


Figure-2: XRD pattern of $Zn_{0.85}Ni_{0.1}Mg_{0.05}Fe_2O_4$ sample.

The lattice parameter (a) and the unit cell volume (V) of $Zn_{0.85}Ni_{0.1}Mg_{0.05}Fe_2O_4$ sample were estimated from (400) plane using the relations [25];

$$a = d\sqrt{h^2 + k^2 + l^2} \quad \text{and}$$

$$V = a^3$$

where 'd' is the inter-planar spacing, 'h,k and l' are Miller indices. The average crystallite size (D) of $Zn_{0.85}Ni_{0.1}Mg_{0.05}Fe_2O_4$ sample was also evaluated from (311) plane using Scherrer's formula [25];

$$D = \frac{0.9\lambda}{\beta \cos \theta}$$

where ' λ ' is the wavelength of Cu $K\alpha$ source ($\lambda = 1.5406 \text{ \AA}$), ' β ' is the FWHM of the diffraction peak and ' θ ' is the Bragg angle of the (311) plane.

The lattice constant value of $Zn_{0.85}Ni_{0.1}Mg_{0.05}Fe_2O_4$ sample is found to be about 0.8342 nm. The unit cell volume of the sample is also found to be about 580.5 (\AA)^3 . This reveals that the obtained lattice parameter and unit cell volume of $Zn_{0.85}Ni_{0.1}Mg_{0.05}Fe_2O_4$ sample are slightly lower than the reported values (8.443 \AA and 601.9 (\AA)^3) of the $ZnFe_2O_4$ compound [26]. The observed variation may be related to the effect of ionic radii of the substituted ions. In the present study, some amount of Zn^{2+} ion (ionic radius, 0.83 \AA) [26] is replaced by Ni^{2+} ion (ionic radius, 0.69 \AA) [27] and Mg^{2+} ion (ionic radius, 0.65 \AA) [26]. Thus, the smaller ionic radii of Ni^{2+} and Mg^{2+} ions causes the reduction of the lattice constant and unit cell volume of $Zn_{0.85}Ni_{0.1}Mg_{0.05}Fe_2O_4$ sample. Similar results were reported earlier by Rahman et al. [26] and Manikandan et al. [26]. The average crystallite size of $Zn_{0.85}Ni_{0.1}Mg_{0.05}Fe_2O_4$ sample is also found to be 51 nm, indicating the formation of the nanocrystalline $Zn_{0.85}Ni_{0.1}Mg_{0.05}Fe_2O_4$ sample using the precursor $Zn(NO_3)_2 \cdot 6H_2O$, $Ni(NO_3)_2 \cdot 6H_2O$, $Mg(NO_3)_2 \cdot 6H_2O$ and $Fe(NO_3)_3 \cdot 9H_2O$ and citric acid as a fuel.

3.2. FT-IR study

Fourier transform infrared spectroscopy is a common technique which is used to detect the metal-oxygen ions stretching and bending vibration in compound. The FT-IR spectral study of $Zn_{0.85}Ni_{0.1}Mg_{0.05}Fe_2O_4$ sample synthesized by sol-gel combustion method at calcination temperature of 950°C for 12 hours was conducted between 300 and 1200 cm^{-1} and the obtained spectrum is shown in Fig. 3. As it is observed in the figure, the obtained FT-IR analysis of $Zn_{0.85}Ni_{0.1}Mg_{0.05}Fe_2O_4$ sample confirms the presence of two strong absorption bands ν_1 and ν_2 which lie in the expected range of cubic spinel-type ferrite. The formation of the two IR bands from $Zn_{0.85}Ni_{0.1}Mg_{0.05}Fe_2O_4$ sample reveals the formation of cubic spinel ferrite material, which is consistency with the obtained XRD analysis.

As it observed in the figure, $Zn_{0.85}Ni_{0.1}Mg_{0.05}Fe_2O_4$ sample shows absorption IR bands at around 561 and 423 cm^{-1} . According to Waldron [28], the high frequency band ν_1 around 561 cm^{-1} and the low frequency band ν_2 around 423 cm^{-1} are attributed to that of tetrahedral and octahedral complexes in the synthesized $Zn_{0.85}Ni_{0.1}Mg_{0.05}Fe_2O_4$ sample, respectively. This variation in the band positions between the characteristic vibrations ν_1 and ν_2 is associated with the shorter bond length of oxygen-metal ions in the tetrahedral site and long bond length of oxygen-metal ions in the octahedral site. As compared with the bands of pure $ZnFe_2O_4$ compound reported by Deraz and Alarifi [29], the absorption bands of $Zn_{0.85}Ni_{0.1}Mg_{0.05}Fe_2O_4$ sample is shifted towards higher wavenumber region. The shifted positions of the absorption bands towards higher wavenumber is associated with the substitution of Mg^{3+} and Ni^{2+} ions into $ZnFe_2O_4$ leads to the decrease in metal-oxygen separation in the tetrahedral and octahedral sites.

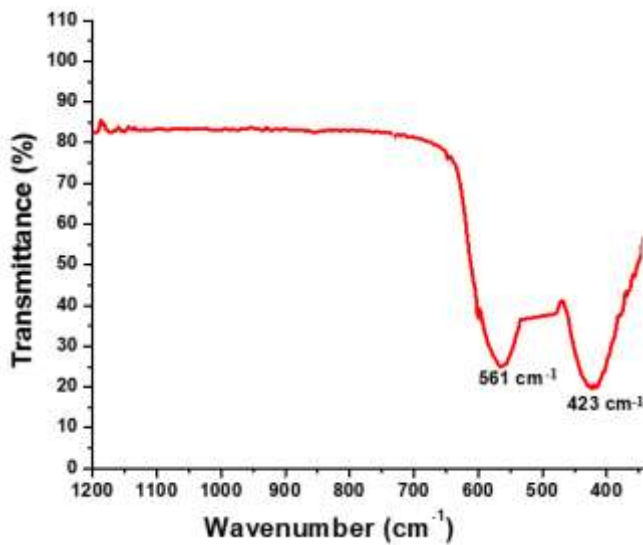
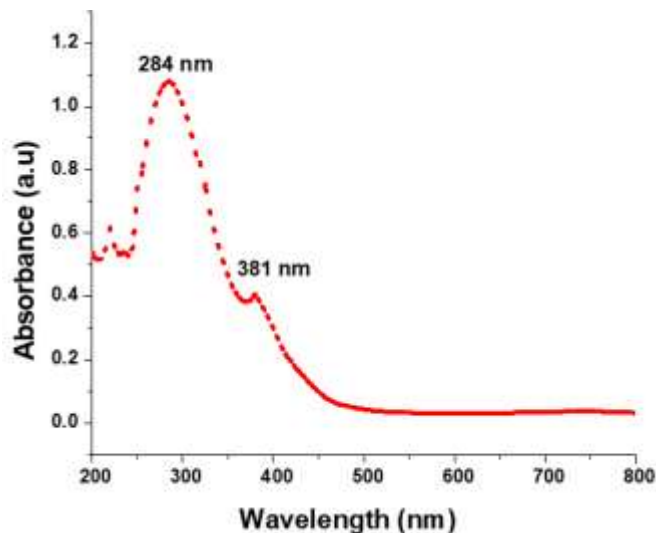


Figure-3: FT-IR spectrum of Zn_{0.85}Ni_{0.1}Mg_{0.05}Fe₂O₄ sample.

3.3. Optical property study

Ultraviolet visible spectroscopy is a very useful characterization to investigate the optical properties like absorption, transmission and reflection of optical materials. It also used to estimate the band gap energy of materials. UV-vis spectroscopy uses electromagnetic radiations between 200 nm to 800 nm and it has two



parts, the first one is an ultraviolet region which covers a wavelength of 200 to 400 nm and the second one is a visible region which covers a wavelength of 400 to 800 nm. In this study, the UV-Vis spectroscopy study was conducted to

Figure-4: UV-vis spectrum of Zn_{0.85}Ni_{0.1}Mg_{0.05}Fe₂O₄ sample.

investigate the optical property as well as to estimate the band gap energy of Zn_{0.85}Ni_{0.1}Mg_{0.05}Fe₂O₄ sample. In this study the UV-vis measurement was conducted in the wavelength range of 200 to 800 nm. Fig. 4 illustrates the

absorbance spectrum of Zn_{0.85}Ni_{0.1}Mg_{0.05}Fe₂O₄ sample synthesized by using sol-gel combustion method at a calcination temperature of 950°C for 12 hours. As shown in the figure, it is identified that Zn_{0.85}Ni_{0.1}Mg_{0.05}Fe₂O₄ sample has high absorbance in the wavelength region of 200 to 284 nm, which decreases gradually as the wavelength increases. The highest absorption spectrum is appeared at a wavelength of around 284 nm, indicating that Zn_{0.85}Ni_{0.1}Mg_{0.05}Fe₂O₄ sample is optically active in the ultraviolet region.

Different researchers were identified that the size of the band gap energy in materials depends on the synthesis method, calcination temperature, crystallite size, lattice parameter and impurities present in the material. The optical band gap energy of Zn_{0.85}Ni_{0.1}Mg_{0.05}Fe₂O₄ sample was estimated using Tauc's relation [30];

$$ahv = A(hv - E_g)^n$$

Where “ α ” is the absorption coefficient, “ $h\nu$ ” is the energy of photon, “ E_g ” is the band gap energy and “ A ” is the absorbance, the exponent $n = 1/2$ and 2 for direct and indirect transition, respectively. The extrapolation of the straight line segment to $(\alpha h\nu)^{1/2} = 0$ at $h\nu$ axis gives the absorption band gap energies for Zn_{0.85}Ni_{0.1}Mg_{0.05}Fe₂O₄ sample. Fig. 5 shows the energy band spectrum of Zn_{0.85}Ni_{0.1}Mg_{0.05}Fe₂O₄ sample. As indicated in the figure, the optical band gap energy of Zn_{0.85}Ni_{0.1}Mg_{0.05}Fe₂O₄ sample is found to be 2.4 eV. The obtained value confirms that Zn_{0.85}Ni_{0.1}Mg_{0.05}Fe₂O₄ sample is a semiconductor material. Moreover, it is also identified that Zn_{0.85}Ni_{0.1}Mg_{0.05}Fe₂O₄ sample processes a direct band gap energy. On the other

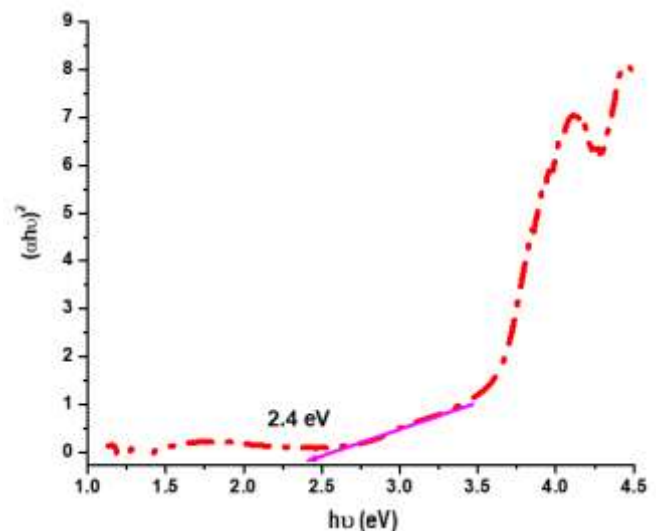


Figure-5: Energy band spectrum of Zn_{0.85}Ni_{0.1}Mg_{0.05}Fe₂O₄ sample.

hand, the obtained band gap energy of $Zn_{0.85}Ni_{0.1}Mg_{0.05}Fe_2O_4$ sample is slightly larger than the reported value (2.15 eV) of the $ZnFe_2O_4$ compound [26], which may be associated with the difference in the crystallite size of both materials.

3. CONCLUSION

$Zn_{0.85}Ni_{0.1}Mg_{0.05}Fe_2O_4$ nanoparticles were successfully synthesized by using a sol-gel combustion method using nitrates salts and citric acid as a fuel and chelating agent. The XRD analysis confirmed a good crystallinity of the synthesized nanoparticles. It also revealed that $Zn_{0.85}Ni_{0.1}Mg_{0.05}Fe_2O_4$ compound possessed a cubic spinel-type structure with Fd-3m space group. The average crystallite size was calculated by Debye Scherrer's formula and it was found to be 51 nm, indicating the formation of nanoparticles in $Zn_{0.85}Ni_{0.1}Mg_{0.05}Fe_2O_4$ sample. The room temperature FTIR spectrum of $Zn_{0.85}Ni_{0.1}Mg_{0.05}Fe_2O_4$ sample confirmed the formation of two strong absorption bands at 561 and 423 cm^{-1} , which were assigned to the stretching vibration of the metal-oxygen bonding force of tetrahedral and octahedral sites, respectively. The calculated optical band gap energy was found to be 2.4 eV, indicating the semiconductor behavior of $Zn_{0.85}Ni_{0.1}Mg_{0.05}Fe_2O_4$ nanoparticles.

ACKNOWLEDGEMENT

The author duly acknowledges Dr. Paulos Tadesse for his support. The author also acknowledges Adama Science and Technology University and Department of Chemistry for conducting XRD, FTIR and UV-vis and characterization.

REFERENCES

- [1] R. N. Bhowmik, N. Naresh, Structure, ac conductivity and complex impedance study of Co_3O_4 and Fe_3O_4 mixed spinel ferrites, International Journal of Engineering, Science and Technology, vv. 2, 2010, pp. 40-52.
- [2] I. Chicinas, Soft magnetic nanocrystalline powders produced by mechanical alloying routes, journal of Optoelectronics and Advanced Materials, vv. 8, 2006, pp. 439-448.
- [3] K. J. Standley, Oxide magnetic materials, 2nd edition, 1972.
- [4] P. P. Hankare, R.P. Patil, U.B. Sankpal, S.D. Jadhav, I.S. Mulla, K.M. Jadhav, B.K. Chougule, Magnetic and dielectric properties of nanophase manganese-substituted lithium ferrite, Journal of Magnetism and Magnetic Materials, vv. 321, 2009, pp. 3270-3273.
- [5] M.A. Elkestawy, S.A. Kader, M.A. Amer, AC conductivity and dielectric properties of Ti-doped $CoCr_{1.2}Fe_{0.8}O_4$ spinel ferrite, Physica B: Condensed Matter, vv. 405, 2010, pp. 619-624.
- [6] S. Soliman, A. Elfalaky, G.H. Fecher, C. Felser, Electronic structure calculations for $ZnFe_2O_4$, Physical Review B, vv. 83, 2011, pp. 085205-1-6.
- [7] G. Sathishkumar, C. Venkataraju, K. Sivakumar, Studies of Nickel Substituted Cobalt-Zinc Ferrite, Materials Science and Applications, vv. 1, 2010, pp. 19-24
- [8] A.M. Bhavikatti, S. kulkarni, A. Lagashetty, Magnetic and transport properties of Cobalt ferrite, International Journal of Electronic Engineering Research, vv. 2, 2010, pp. 125-134.
- [9] P.I. Slick, Ferrites for Non-Microwave Applications" North Holland, Amsterdam, Vol. 2, 1980.
- [10] E. J. W. Verwey, and E.L. Heilman, Physical Properties and Cation Arrangement of Oxides with Spinel Structures I. Cation Arrangement in Spinel, the journal of Chemical Physics, vv. 15, 1947, pp. 174.
- [11] F.S. Li, H.B. Wang, L. Wang, J.B. Wang, Magnetic properties of $ZnFe_2O_4$ nanoparticles produced by a low-temperature solid-state reaction method, Journal of Magnetism and Magnetic Materials, vv. 309, 2007, pp. 295-299.
- [12] R.K. Selvan, V. Krishnan, C.O. Augustin, H. Bertagnolli, C.S. Kim, S. Gedanken, Investigations on the structural, morphological, electrical, and magnetic properties of $CuFe_2O_4$ - NiO nanocomposites, Chemistry of Materials, vv. 20, 2008, pp. 429-439
- [13] N. Ponpandian, A. Narayanasamy, Influence of grain size and structural changes on the electrical properties of nanocrystalline zinc ferrite, Journal of Applied Physics, vv. 92, 2002, pp. 2770-2778.
- [14] W.Q. Meng, F. Li, D.G. Evans, X. Duan, Photocatalytic activity of highly porous zinc ferrite prepared from a zinc-iron (III)-sulfate layered double hydroxide precursor, Journal of Porous Materials, vv. 11, 2004, pp. 97-105.
- [15] T.E. Quickel, V.H. Le, T. Brezesinski, S.H. Tolbert, On the correlation between nanoscale structure and magnetic properties in ordered mesoporous cobalt ferrite ($CoFe_2O_4$) thin film, Nano Letter, vv. 10, 2010, pp. 2982-2988.
- [16] G. Fan, Z. Gu, L. Yang, F. Li, Nanocrystalline zinc ferrite photocatalysts formed using the colloid mill and hydrothermal technique, Chemical Engineering Journal, vv. 155, 2009, pp. 534-541.
- [17] C. Zhou, T.C. Schulthess, D.P. Landau Monte carlo, Simulations of $NiFeO$ nanoparticles, Journal of Applied Physics, vv. 99, 2006, pp. 08H906-08H906-3
- [18] N. Millot, S. L. Gallet, D. Aymes, F. Bernard, F. Grin, Spark plasma sintering of cobalt ferrite nanopowders prepared by coprecipitation and hydrothermal synthesis, Journal of the European Ceramic Society, vv. 27, 2007, pp. 921-926.
- [19] T.A.S. Ferreira, J. C. Waerenborgh, M.H.R.M, M. R. Nunes, F. M. Costaa, Structural and morphological characterization of $FeCo_2O_4$ and $CoFe_2O_4$ spinels prepared by a coprecipitation method, Solid State Science, pp. 5, 2003, pp. 383-392.

- [20] D.Q. Tang, D.J. Zang, H Ai, Fabrication of Magnetic Core-Shell $\text{CoFe}_2\text{O}_4/\text{Al}_2\text{O}_3$ Nanoparticles as Immobilized Metal Chelate Affinity Support for Protein Adsorption, *Chemistry Letters*, vv. 35, 2006, pp. 1238-1239.
- [21] M.K. Shobana, V. Rajendran, M. Jeyasubramanian, N. S. Kumar, Preparation and characterisation of NiCo ferrite nanoparticles, *Materials Letter*, vv. 61, 2007, pp. 2616-2619.
- [22] S. Nasir and M. Anis-ur-Rehman, Structural, electrical and magnetic studies of nickel-zinc nanoferrites prepared by simplified sol-gel and co-precipitation methods, *physica Script*, vv, 84, 2011, pp. 025603-1-7.
- [23] J. Grabis, I. Zalite, Nanosized Powders of Refractory Compounds for Obtaining of Fine-Grained Ceramic Materials, *Material Science Forum*, vv. 555, 2007, pp. 267-272.
- [24] S. Rahman, K. Nadeem, M. Anis-ur-Rehman, M. Mumtaz, S. Naeem, I. Letofsky-Papst, Structural and magnetic properties of ZnMg-ferrite nanoparticles prepared using the co-precipitation method, *Ceramics International*, vv. 39, 2013, pp. 5235-5239.
- [25] M. Srivastava, A.K. Ojha, S. Chaubey, A. Materny, Synthesis and optical characterization of nanocrystalline NiFe_2O_4 structures, *Journal of Alloys and Compounds*, vv. 481, 2009, pp. 515-519.
- [26] A. Manikandan, J. Judith Vijaya, M. Sundararajan, C. Meganathan, L. John Kennedy, M. Bououdina, Optical and magnetic properties of Mg-doped ZnFe_2O_4 nanoparticles prepared by rapid microwave combustion method, *Superlattices and Microstructures*, vv. 64, 2013, 118-131.
- [27] Y. Qu, H. Yang, N. Yang, The effect of reaction temperature on the particle size, structure and magnetic properties of co-precipitated CoFe_2O_4 nanoparticles, *Materials Letters*, vv. 60, 2006, pp. 3548-3552
- [28] R.D. Waldron, Evaluation of ac conductivity & dielectric behavior of cobalt ferrite, *Physical Review*, vv. 99, 1955, pp. 1727-1735.
- [29] N.M. Deraz, A. Alarifi, Synthesis and characterization of pure and Li_2O doped ZnFe_2O_4 nanoparticles via glycine assisted route, *Polyhedron*, vv. 28, 2009, pp. 4122-4130.
- [30] G.P. Joshi, N.S.Saxena, R.Mangal, A.Mishra and T.P.Sharma. Band gap determination of Ni-Zn ferrites. *Journal of Indian Academy of Sciences*, vv. 26, 2003, pp. 387-389.